International Journal of Pressure Vessels and Piping 182 (2020) 104065

Contents lists available at ScienceDirect

International Journal of Pressure Vessels and Piping

journal homepage: http://www.elsevier.com/locate/ijpvp

Radially symmetric response of an FGM spherical pressure vessel under thermal shock using the thermally nonlinear Lord-Shulman model

P. Karimi Zeverdejani [a], Y. Kiani [b,*]

[a] Mechanical Engineering Department, Shahrekord University, Shahrekord, Iran
[b] Faculty of Engineering, Shahrekord University, Shahrekord, Iran

ARTICLE INFO

Keywords:
Exponentially graded
Functionally graded
Hollow sphere
Lord-Shulman theory
Newmark time marching method
Thermal shock

ABSTRACT

In the present research, the coupled and non-linear thermo-mechanical response of a functionally graded material (FGM) hollow sphere under thermal shock is investigated. It is assumed that all of the properties of the sphere except for the thermal relaxation time are graded through the radial direction using an exponential representation. The formulation is based on the Lord and Shulman theory which contains a single relaxation time parameter to avoid the infinite speed of temperature wave propagation. Two coupled equations namely energy and motion equations are obtained. These two equations are written in terms of temperature change and radial displacement. The energy equation is kept in its non-linear form and the assumption of small temperature change in comparison to reference temperature is not established in this research. The obtained equations are provided in a dimensionless presentation. After that using the generalised differential quadrature (GDQ) method, nonlinear algebraic presentation of the governing equations is established. Using the successive Picard algorithm and the Newmark time marching scheme, the temporal evolution of the temperature and displacement are obtained. Numerical results are validated for the case of homogeneous sphere with the available data in the open literature. After that, novel numerical results are given to explore the effect of relaxation time, coupling parameter, exponential index and non-linearity of the energy equation.

1. Introduction

Response of Hollow spheres under thermal or mechanical shock has been the subject of many studies within the last decades [1–3]. In most of the works, it is postulated that temperature change is infinitesimal in comparison to the reference temperature. As a result, the energy equation may be linearised and the governing equations are linear. Among the works dealing with the generalised thermoelasticity of functionally graded material (FGM) hollow spheres with different second sound theories the following works may be mentioned.

Kar and Kanoria [4] applied the three phase lag theory to investigate the propagation of thermal and mechanical waves in an FGM spherical body with orthotropic properties. With the aid of the Laplace transformation technique, the basic equations are provided in the transformed domain. The eigenvalue approach is used to solve the transformed equations in a vector-matrix presentation. Various theories such as the Green-Naghdi type II and Green-Naghdi type III may be obtained as especial cases. Also the case of a body with spherical cavity may be investigated as an especial case. Shariyat et al. [5] obtained the response of FGM hollow spheres subjected to thermal and mechanical shock in ambient moisture. The formulation is within the framework of Lord and Shulman theory of generalised thermoelasticity which accounts for a single relaxation time. The Galerkin type of finite elements formulation which is applicable directly to the governing equations is adopted to discretize the governing coupled and non-linear equations. The strain rate effects are also included in the present research. To guarantee the exact continuity of the stresses at the mutual boundaries of the elements, C1 Hermitian elements are adopted. It is verified that in an FGM sphere the speed of propagation of temperature and stress waves is non-uniform within the body. For a functionally graded hollow sphere which is reinforced with non-uniform distribution of graphene platelets (GPLs) Heydarpour et al. [6] obtained the propagation of waves using the Lord-Shulman theory. In this research, the effective elastic properties of the media are calculated using the Halpin-Tsai approach. Laplace transformation technique is used to deal with the time dependency of the governing equations. Multi-step time integration scheme based on the non-uniform rational B-spline (NURBS) in conjunction with Newton-Raphson algorithm are employed to solve the coupled and

* Corresponding author.
E-mail address: y.kiani@sku.ac.ir (Y. Kiani).

https://doi.org/10.1016/j.ijpvp.2020.104065
Received 28 December 2019; Received in revised form 10 February 2020; Accepted 13 February 2020
Available online 19 February 2020
0308-0161/© 2020 Elsevier Ltd. All rights reserved.

nonlinear equations in algebraic form. It is shown that the speed of waves is highly dependent to the amount of GPLs within the body. Banik and Kanoria [7] investigated the response of an infinite body with spherical cavity using the three phase lag theory of thermo-elasticity. The heat conduction equation in this theory is a hyperbolic equation which admits the finite speed of temperature wave in the body. Specific attention is devoted to the special case of Green-Naghdi type II which is without energy dissipation and Green Naghti type III which admits the energy dissipation. A unified generalised thermoelasticity theory is developed by Bagri and Eslami [8] to analyse the propagation, reflection and interaction of thermal and mechanical waves in hollow spheres. Auxiliary parameters are introduced to unify the well-known thermo--elasticity theories such as Lord-Shulman theory, Green-Lindsay theory and Green-Naghdi theory. Using the Laplace transformation technique in time domain and the Galerkin type of finite elements in radial direction of the sphere, the equations are discretized and solved. It is highlighted that under each of these theories, temperature wave propagates with finite speed. Using the classical coupled thermoelasticity formulation which admits the thermal-structural coupling and ignores the finite speed of temperature wave, Shahani and Momeni Bashusqeh obtained the response of homogeneous hollow spheres under mechanical [9] or transient thermal shock [10]. In the mentioned works, finite Hankel transformation technique is employed to obtain the response of the sphere under thermal and/or mechanical shocks. Closed form expressions are obtained in each case to investigate the propagation of thermal and mechanical waves in the spherical bodies. Povstenko [11] investigated the response of a hollow sphere within the framework of fractional theory of thermo-elasticity. Caputo time-fractional derivative with positive order smaller than two is established. The solution is obtained applying Laplace and finite sine-Fourier integral transforms. The Dirichlet problem with the prescribed boundary value of the temperature is considered. He also developed the formulation for the case of a sphere under heat flux [12]. Sur and Kanoria [13] developed the thermal stresses and temperature profile within a spherical body made of visco-elastic materials. Using the Laplace transformation technique and Bellman numerical inversion, the magnitude of temperature, displacement and stresses are obtained as time evolutes.

As the above literature survey reveals, most of the investigations deal with the linear formulation of generalised thermoelasticity of hollow spheres where temperature change is negligible in comparison to reference temperature. In the present investigation, the thermally nonlinear formulation is adopted which is originated from the assumption that temperature change is comparable with respect to reference temperature. Under the Lord and Shulman theory assumption, two coupled equations are established as the energy and motion equations. These equations for a hollow sphere made of an exponentially graded media are provided in a dimensionless presentation. After that, using the GDQ method, Newmark time marching scheme and Picard successive algorithm, the equations are solved to obtain the temperature, displacement and stresses within the body as a function of time. Results are devoted to explore the effects of coupling parameter, relaxation time and non-linearity.

2. Functionally graded sphere

A hollow sphere is considered in the current research which is made from a functionally graded material. The inner and outer radii of the hollow sphere are denoted by a and b, respectively. Radial coordinate r is measured from the center of the sphere. In the present research, it is assumed that properties of the sphere except for the Poisson ratio ν and thermal relaxation time t_0 are graded through the radial direction using an exponential presentation. Thus, a thermo-mechanical property, P may be considered in the form

$$P(r) = P_0 e^{\lambda_P \frac{r-a}{b-a}} \tag{1}$$

In Eq. (1), P_0 stands for the property at the inner radius of the sphere and the property at the outer radius of the sphere is evaluated as $P_0 e^{\lambda_P}$ where λ_P is the exponential inhomogeneity index of the FGM media.

It is assumed that elasticity modulus, E, thermal expansion coefficient, α, thermal conductivity, K, mass density, ρ and specific heat C_ε follow the representation (1).

3. Equation of motion

An FGM hollow sphere which is subjected to the radially symmetric thermal loads on the boundaries is assumed in this research. Under the assumption of radially symmetric loading and boundary conditions, the response of the hollow sphere is also radially symmetric. Under such conditions, two of the equations of motion vanish and only the radial one remains. Since circumferential and azimuthal components of the stress and strain are the same in radially symmetric conditions, the equation of motion takes the form[14].

$$\frac{\partial \sigma_{rr}}{\partial r} + \frac{2(\sigma_{rr} - \sigma_{\varphi\varphi})}{r} = \rho(r)\frac{\partial^2 u}{\partial t^2} \tag{2}$$

In Eq. (2) σ_{rr} and $\sigma_{\varphi\varphi}$ are the radial and azimuthal(circumferential) stresses. Also u stands for the radial displacement in the hollow sphere. Furthermore t stands for time.

For the case of radially symmetric deformations in the sphere, the stress components may be expressed in terms of strains and temperature change as

$$\begin{aligned} \sigma_{rr} &= \frac{E(r)}{(1-2\nu)(1+\nu)}\left((1-\nu)\varepsilon_{rr} + 2\nu\varepsilon_{\varphi\varphi} - (1+\nu)\alpha(r)\theta(r)\right) \\ \sigma_{\varphi\varphi} &= \frac{E(r)}{(1-2\nu)(1+\nu)}\left(\varepsilon_{\varphi\varphi} + \nu\varepsilon_{rr} - (1+\nu)\alpha(r)\theta(r)\right) \end{aligned} \tag{3}$$

In Eq. (3), $\theta(r)$ stands for the temperature change in the sphere which may be replaced by $\theta(r) = T(r) - T_0$. Here $T(r)$ is temperature in the body and T_0 is reference temperature. Also ε_{rr} and $\varepsilon_{\varphi\varphi}$ are the radial and azimuthal(circumferential) normal strains, respectively.

Strain components for the case of radially symmetric deformations are obtained easily in terms of the radial displacement as

$$\begin{aligned} \varepsilon_{rr} &= \frac{\partial u}{\partial r} \\ \varepsilon_{\varphi\varphi} &= \frac{u}{r} \end{aligned} \tag{4}$$

The radial equation of motion in terms of radial displacement and temperature change may be obtained easily when Eqs. (3) and (4) are inserted into Eq. (2). With the aid of Eq. (1) which is used in here to obtain the distribution of elasticity modulus and thermal expansion coefficient, one may reach to

$$\begin{aligned} &\frac{1-\nu}{(1+\nu)(1-2\nu)}E\left(r\right)\left(\frac{\partial^2 u}{\partial r^2} + \left(\frac{\lambda_E}{c} + \frac{2}{r}\right)\frac{\partial u}{\partial r} + 2\left(\frac{\lambda_E \nu}{c(1-\nu)}r - 1\right)\frac{u}{r^2} - \right. \\ &\left.\frac{1+\nu}{1-\nu}\left(\frac{\lambda_E + \lambda_\alpha}{c}\right)\alpha\left(r\right)\theta\left(r\right) - \frac{1+\nu}{1-\nu}\alpha\left(r\right)\frac{\partial \theta}{\partial r}\right) = \rho(r)\frac{\partial^2 u}{\partial t^2} \end{aligned} \tag{5}$$

where in Eq. (5) $c = b - a$.

4. Energy equation

As known, in the developed theory by Lord and Shulman, an auxiliary parameter known as the relaxation time is introduced which modifies the Fourier law of heat conduction as [14].

$$q + t_0\dot{q} = -K(r)\frac{\partial T}{\partial r} \tag{6}$$

In Eq. (6) q represents the radial heat flux and $K(r)$ stands for the position-dependent thermal conductivity.

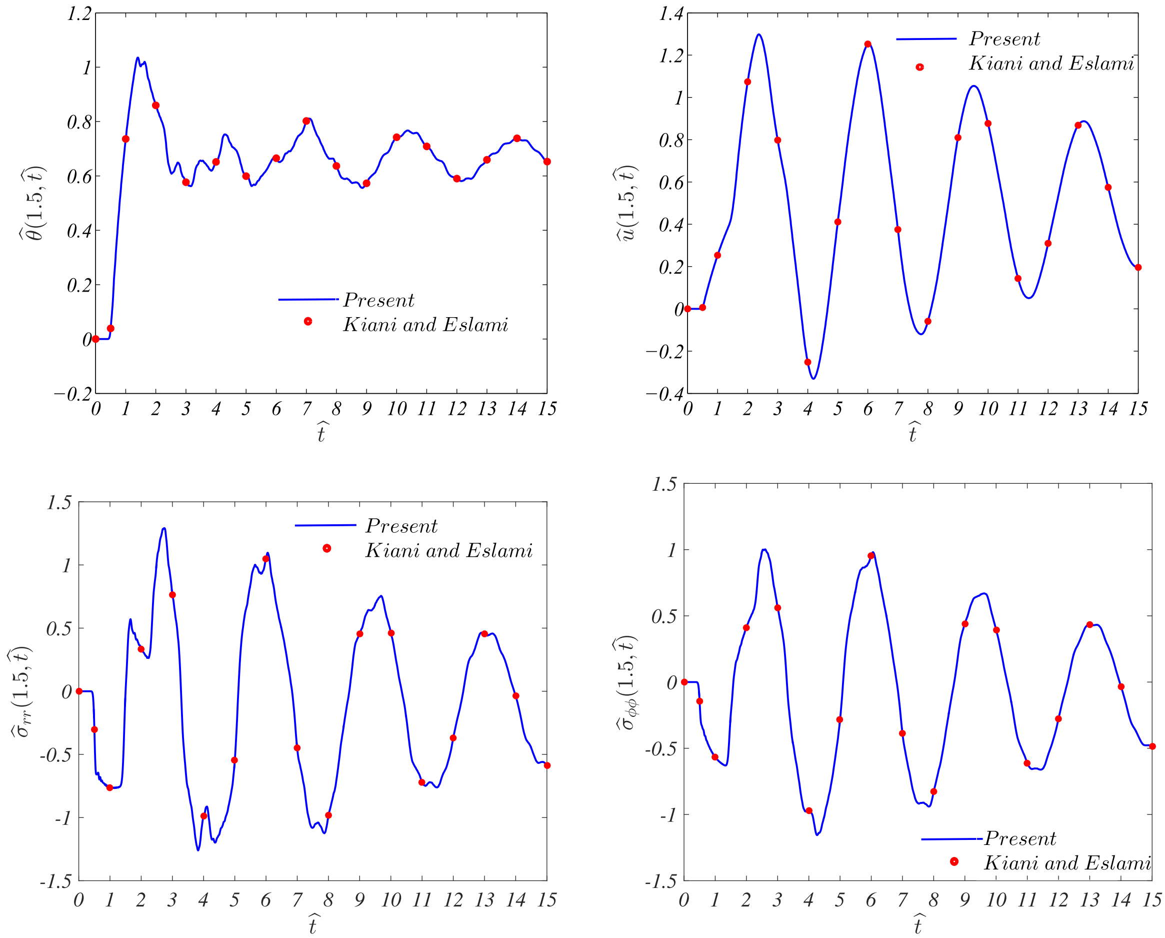

Fig. 1. A comparison of nonlinear temporal evolution of dimensionless radial displacement, temperature, radial and hoop stresses at $\hat{r} = 1.5$ between the results of this study and those of Kiani and Eslami [30] for $\hat{t}_0 = 1$, $A = 0.02111$ and $\hat{q}_{in} = 4$.

In spherical coordinates, the heat balance for an element which provides the radial heat flux q in terms of rate of specific heat influx Q may be expressed as [15].

$$\dot{Q} = -\frac{1}{r^2}\frac{\partial(r^2 q)}{\partial r} \tag{7}$$

The differential presentation of the second law of the thermodynamics takes the form

$$\delta Q = TdS \tag{8}$$

Considering the temperature, radial strain, circumferential strain and azimuthal strain as distinct variables, Eq. (8) in rate form takes the form

$$\dot{Q} = T\dot{S} = T\left(\frac{\partial S}{\partial \varepsilon_{rr}}\dot{\varepsilon}_{rr} + \frac{\partial S}{\partial \varepsilon_{\varphi\varphi}}\dot{\varepsilon}_{\varphi\varphi} + \frac{\partial S}{\partial \varepsilon_{\theta\theta}}\dot{\varepsilon}_{\theta\theta} + \frac{\partial S}{\partial T}\dot{T}\right) \tag{9}$$

which simplifies to

$$\dot{Q} = \frac{1}{1-2\nu}E(r)\alpha(r)T(r)\dot{\varepsilon}_{rr} + \frac{2}{1-2\nu}E(r)\alpha(r)T(r)\dot{\varepsilon}_{\varphi\varphi} + \rho(r)C_\varepsilon(r)\dot{T} \tag{10}$$

Equations (6), (7) and (10) may be combined together to obtain a single equation which is the energy equation compatible with the Lord-Shulman assumptions in polar coordinates as

$$K(r)\left(\frac{\partial^2 T}{\partial r^2} + \left(\frac{2}{r} + \frac{\lambda_K}{c}\right)\frac{\partial T}{\partial r}\right) - \frac{1}{1-2\nu}E(r)\alpha(r)\left(1 + t_0\frac{\partial}{\partial t}\right)(\dot{\varepsilon}_{rr} + 2\dot{\varepsilon}_{\varphi\varphi}) - \left(1 + t_0\frac{\partial}{\partial t}\right)C_\varepsilon(r)\rho(r)\dot{T} = 0 \tag{11}$$

With substitution of Eq. (4) into Eq. (11) the following energy equation is revealed

$$K(r)\left(\frac{\partial^2 T}{\partial r^2} + \left(\frac{2}{r} + \frac{\lambda_K}{c}\right)\frac{\partial T}{\partial r}\right) - \frac{1}{1-2\nu}E(r)\alpha(r)T\left(\frac{\partial^2 u}{\partial t\partial r} + \frac{2}{r}\frac{\partial u}{\partial t}\right) - \frac{1}{1-2\nu}t_0E(r)\alpha(r)\frac{\partial T}{\partial t}\left(\frac{\partial^2 u}{\partial t\partial r} + \frac{2}{r}\frac{\partial u}{\partial t}\right) - \frac{1}{1-2\nu}E(r)\alpha(r)t_0T\left(\frac{\partial^3 u}{\partial t^2\partial r} + \frac{2}{r}\frac{\partial u}{\partial t^2}\right) - C_\varepsilon(r)\rho(r)\left(\frac{\partial T}{\partial t} + t_0\frac{\partial^2 T}{\partial t^2}\right) = 0 \tag{12}$$

As seen, Eq. (12) is a non-linear equation since the temperature/temperature rate is multiplied by the strains and their derivatives. Generally this equation is simplified when the temperature change is assumed to be negligible in comparison to the reference temperature. Substitution of T by $T_0 + \theta$ in Eq. (12) results in

$$K(r)\left(\frac{\partial^2\theta}{\partial r^2}+\left(\frac{2}{r}+\frac{\lambda_K}{c}\right)\frac{\partial\theta}{\partial r}\right)-\frac{1}{1-2\nu}E(r)\alpha(r)T_0\left(1+\frac{\theta}{T_0}\right)\left(\frac{\partial^2 u}{\partial t\partial r}+\frac{2}{r}\frac{\partial u}{\partial t}\right)- \frac{1}{1-2\nu}t_0E(r)\alpha(r)\frac{\partial\theta}{\partial t}\left(\frac{\partial^2 u}{\partial t\partial r}+\frac{2}{r}\frac{\partial u}{\partial t}\right)-\frac{1}{1-2\nu}E(r)\alpha(r)t_0T_0\left(1+\frac{\theta}{T_0}\right)\left(\frac{\partial^3 u}{\partial t^2\partial r}+\frac{2}{r}\frac{\partial u}{\partial t^2}\right)- C_\varepsilon(r)\rho(r)\left(\frac{\partial\theta}{\partial t}+t_0\frac{\partial^2\theta}{\partial t^2}\right)=0 \tag{13}$$

When the assumption of small temperature change in comparison to reference temperature is established the following energy equation is achieved

$$K(r)\left(\frac{\partial^2\theta}{\partial r^2}+\left(\frac{2}{r}+\frac{\lambda_K}{c}\right)\frac{\partial\theta}{\partial r}\right)-\frac{1}{1-2\nu}E(r)\alpha(r)T_0\left(\frac{\partial^2 u}{\partial t\partial r}+\frac{2}{r}\frac{\partial u}{\partial t}\right)- \frac{1}{1-2\nu}E(r)\alpha(r)t_0T_0\left(\frac{\partial^3 u}{\partial t^2\partial r}+\frac{2}{r}\frac{\partial u}{\partial t^2}\right)-C_\varepsilon(r)\rho(r)\left(\frac{\partial\theta}{\partial t}+t_0\frac{\partial^2\theta}{\partial t^2}\right)=0 \tag{14}$$

In this study, the phrase *thermally nonlinear* indicates the nonlinearity arising from the existence of T in the energy equation (12). On the other hand, the linear analysis is dominant when the analysis is performed by Eq. (14) where the temperature change is assumed to be negligible in comparison to reference temperature.

5. Equations in non-dimensional form

In this section, the basic equations (5) and (12) which are the motion and energy equations are provided in dimensionless presentation for the sake of generality. For this aim, the following dimensionless parameters are introduced. Eqs (5) and (12) are transformed into the dimensionless form with the introduction of the following non-dimensional variables

$$\begin{aligned}&\widehat{r}=\frac{r}{l_0},\ \widehat{a}=\frac{a}{l_0},\ \widehat{b}=\frac{b}{l_0}\\&\widehat{t}=\frac{C_{e_0}}{l_0}t,\ \widehat{t}_0=\frac{C_{e_0}}{l_0}t_0,\\&\widehat{\theta}=\frac{\theta}{T_0},\ \widehat{q}=\frac{l_0}{K_0T_0}q\\&\widehat{u}=\frac{1-\nu}{l_0\alpha_0T_0(1+\nu)}u,\ \widehat{\sigma}_{rr}=\frac{1-2\nu}{E_0\alpha_0T_0}\sigma_{rr},\ \widehat{\sigma}_{\varphi\varphi}=\frac{1-2\nu}{E_0\alpha_0T_0}\sigma_{\varphi\varphi},\end{aligned} \tag{15}$$

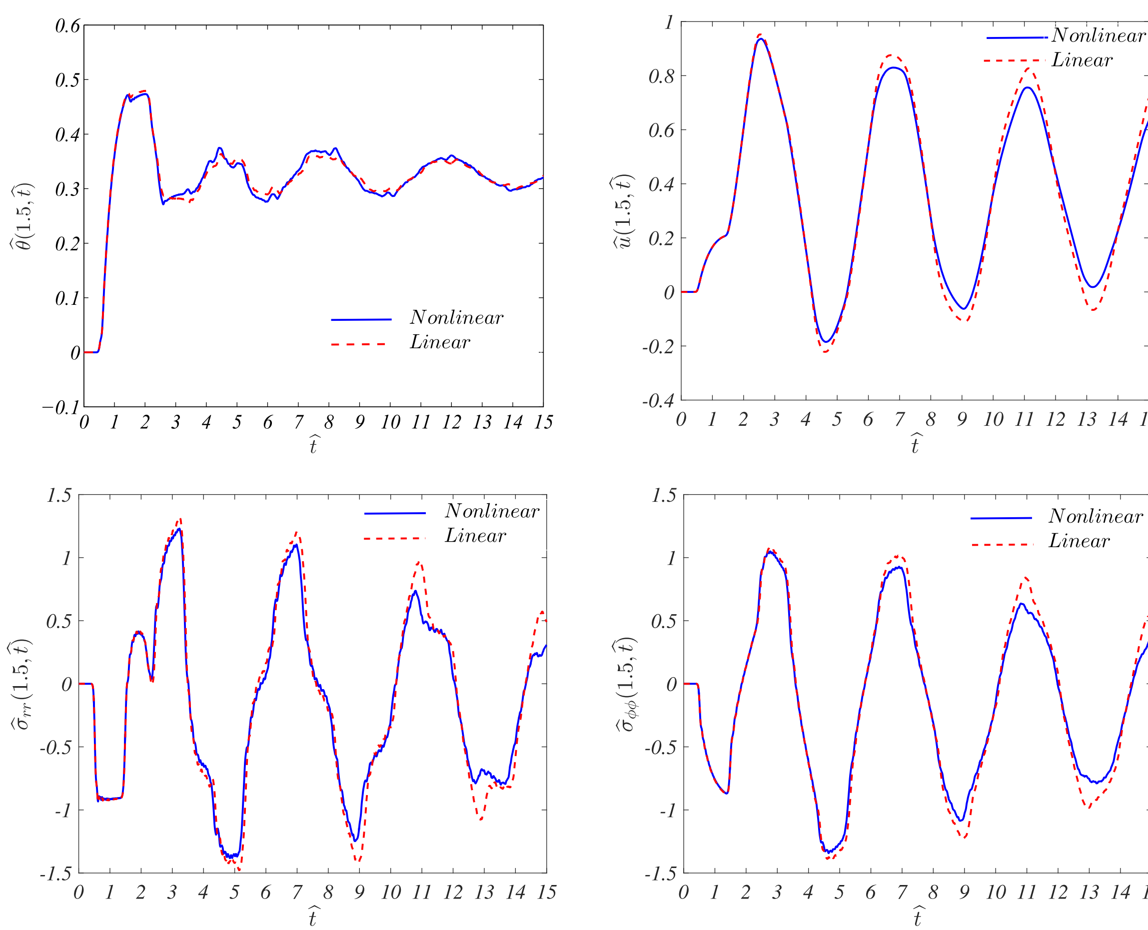

Fig. 2. Linear and nonlinear temporal evolution of dimensionless radial displacement, temperature, radial and hoop stresses at $\widehat{r}=1.5$ of an FGM hollow sphere with $\widehat{t}_0=1$, $A=0.02111$, $\lambda=1$ and $\widehat{q}_{in}=4$.

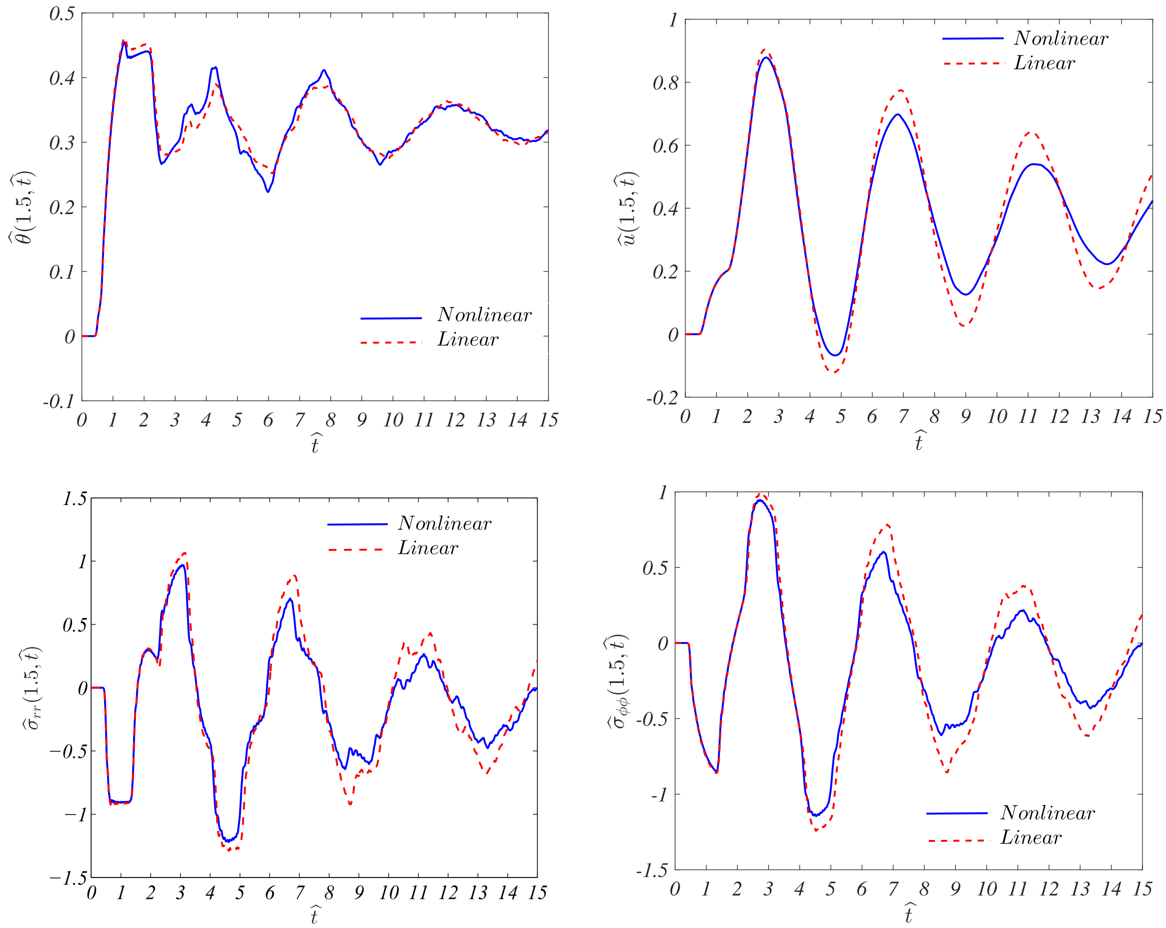

Fig. 3. Linear and nonlinear temporal evolution of dimensionless radial displacement, temperature, radial and hoop stresses at $\hat{r} = 1.5$ of an FGM hollow sphere with $\hat{t}_0 = 1$, $A = 0.05$, $\lambda = 1$ and $\hat{q}_{in} = 4$.

In Eq. (15) a symbol ^ is used to show the dimensionless parameter. Parameter l_0 is a characteristic length which is defined by. $l_0 = K_0(\rho_0 C_{\epsilon 0} C_{e0})^{-1}$

Here C_{e0} is the classical speed of elastic wave propagation in the spherical domains which is defined by

$$C_{e0} = \sqrt{\frac{(1-\nu)E_0}{(1+\nu)(1-2\nu)\rho_0}} \tag{16}$$

With the aid of Eq. (15), the equation of motion Eq. (5) and energy equation (12) take the following form in a dimensionless presentation

$$\begin{aligned}
&\frac{\partial^2 \hat{u}}{\partial \hat{r}^2} + \left(\frac{2}{\hat{r}} + \frac{\lambda_E}{\hat{c}}\right)\frac{\partial \hat{u}}{\partial \hat{r}} + 2\left(\frac{\lambda_E \nu \hat{r}}{\hat{c}(1-\nu)} - 1\right)\frac{\hat{u}}{\hat{r}^2} - e^{\lambda_\alpha \frac{\hat{r}-\hat{a}}{\hat{c}}}\left(\frac{\partial \hat{\theta}}{\partial \hat{r}} + \frac{\lambda_E + \lambda_\alpha}{\hat{c}}\hat{\theta}\right) - e^{(\lambda_\rho - \lambda_E)\frac{\hat{r}-\hat{a}}{\hat{c}}}\frac{\partial^2 \hat{u}}{\partial \hat{t}^2} = 0 \\
&\frac{\partial^2 \hat{\theta}}{\partial \hat{r}^2} + \left(\frac{2}{\hat{r}} + \frac{\lambda_K}{\hat{c}}\right)\frac{\partial \hat{\theta}}{\partial \hat{r}} - (1+\hat{\theta})Ae^{(\lambda_E+\lambda_\alpha-\lambda_K)\frac{\hat{r}-\hat{a}}{\hat{c}}}\left(\frac{\partial^2 \hat{u}}{\partial \hat{r}\,\partial \hat{t}} + \frac{2}{\hat{r}}\frac{\partial \hat{u}}{\partial \hat{t}} + \hat{t}_0\frac{\partial^3 \hat{u}}{\partial \hat{t}^2\,\partial \hat{r}} + \hat{t}_0\frac{2}{\hat{r}}\frac{\partial^2 \hat{u}}{\partial \hat{t}^2}\right) - \\
&\hat{t}_0 A e^{(\lambda_E+\lambda_\alpha-\lambda_K)\frac{\hat{r}-\hat{a}}{\hat{c}}}\frac{\partial \hat{\theta}}{\partial \hat{t}}\left(\frac{\partial^2 \hat{u}}{\partial \hat{r}\,\partial \hat{t}} + \frac{2}{\hat{r}}\frac{\partial \hat{u}}{\partial \hat{t}}\right) - e^{\left(\lambda_{C_\epsilon}+\lambda_\rho-\lambda_K\right)\frac{\hat{r}-\hat{a}}{\hat{c}}}\frac{\partial \hat{\theta}}{\partial \hat{t}} - \hat{t}_0 e^{\left(\lambda_{C_\epsilon}+\lambda_\rho-\lambda_K\right)\frac{\hat{r}-\hat{a}}{\hat{c}}}\frac{\partial^2 \hat{\theta}}{\partial \hat{t}^2} = 0
\end{aligned} \tag{17}$$

As mentioned earlier, the parameters which have a symbol ^ in Eq. (17) are dimensionless quantities. The thermally linear analysis takes place, when reference temperature is ignorable in comparison to reference temperature or equivalently $1 + \hat{\theta}$ is approximated by 1.

When the relaxation time $\hat{t}_0$ is set equal to zero, the second equation simplifies to the classical coupled thermoelasticity formulation. It is obvious that, for non-zero values of $\hat{t}_0$ a hyperbolic energy equation is obtained which results in the finite speed of temperature wave. On the other hand, for zero values of $\hat{t}_0$ parabolic equation of energy is obtained which results in the infinite speed of temperature wave.

Also in Eq. (17), the coefficient A is produced in the process of

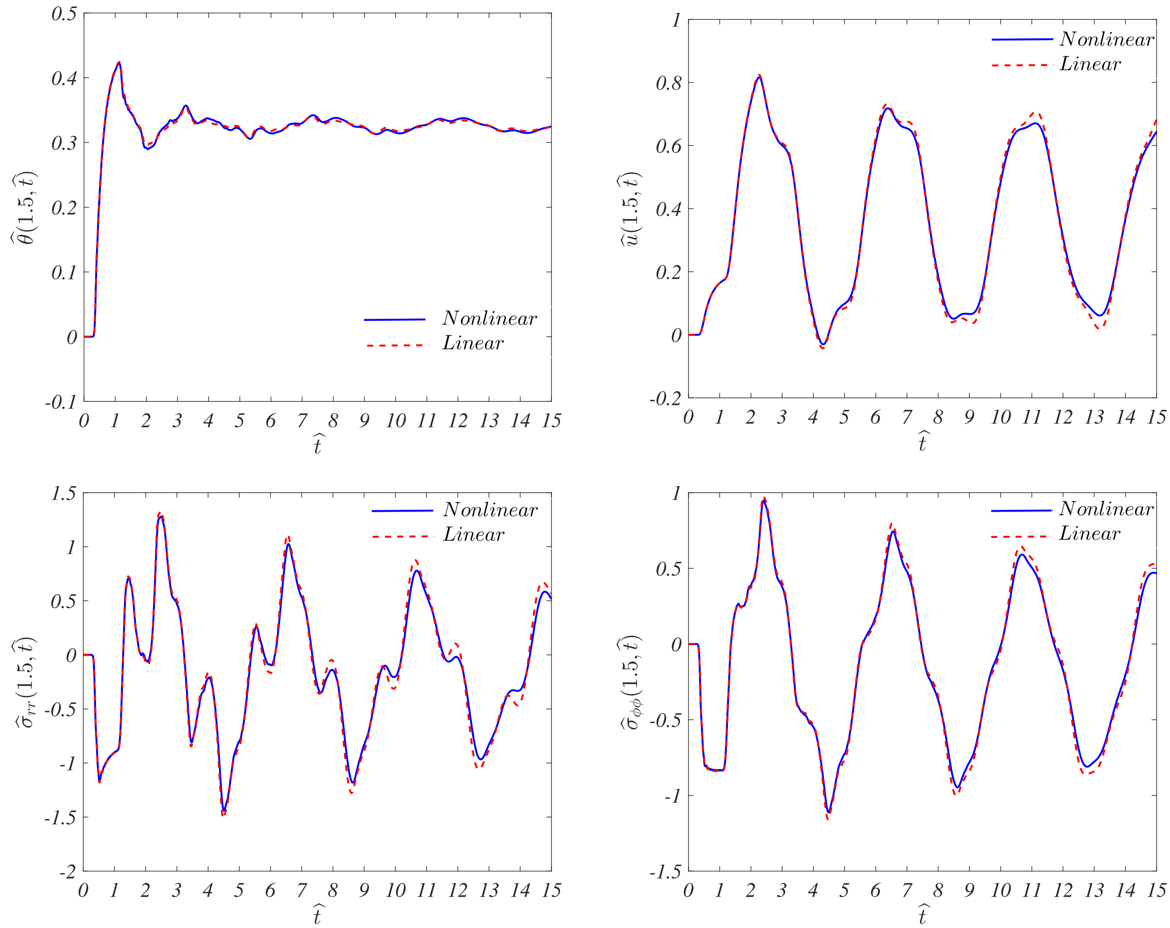

Fig. 4. Linear and nonlinear temporal evolution of dimensionless radial displacement, temperature, radial and hoop stresses at $\hat r = 1.5$ of an FGM hollow sphere with $\hat t_0 = 0.36$, $A = 0.02111$, $\lambda = 1$, and $\hat q_{in} = 4$.

transferring the equation into dimensionless form and indicates the coupling effect for a sphere made of isotropic homogeneous material. This coefficient is equal to

$$A = \frac{T_0 E_0 \alpha_0^2 (1+\nu)}{\rho_0 C_{\varepsilon 0}(1-2\nu)(1-\nu)} \tag{18}$$

When the coupling parameter A is set equal to zero, the uncoupled thermo-elasticity formulation is achieved. Under such conditions, the temperature profile is obtained first and then the extracted temperature profile is inserted into the equation of motion.

Similarly, the components of stress field in a dimensionless presentation take the following form

$$\begin{aligned} \hat\sigma_{rr} &= e^{\lambda_E \frac{\hat r - \hat a}{\hat c}} \left(\frac{\partial \hat u}{\partial \hat r} + \frac{2\nu}{1-\nu}\frac{\hat u}{\hat r} - e^{\lambda_\alpha \frac{\hat r - \hat a}{\hat c}} \hat\theta \right) \\ \hat\sigma_{\varphi\varphi} &= e^{\lambda_E \frac{\hat r - \hat a}{\hat c}} \left(\frac{1}{1-\nu}\frac{\hat u}{\hat r} + \frac{\nu}{1-\nu}\frac{\partial \hat u}{\partial \hat r} - e^{\lambda_\alpha \frac{\hat r - \hat a}{\hat c}} \hat\theta \right) \end{aligned} \tag{19}$$

6. Solution method

Equation (17) interpret two coupled equations in terms of dimensionless temperature change and radial displacement in a hollow sphere made of FGMs subjected to thermal shock. These equations are coupled and non-linear due to the assumptions made in the previous sections. Therefore, exact solution of such equations even if exists is complicated. A numerical solution is needed to obtain the profiles of radial displacement and temperature change at each time step. Different numerical methods are used in the open literature to solve the governing equations of solids and structures, for instance finite element method [16,17], discrete singular convolution method [18–21], asymptotic iteration method [22], harmonic differential quadrature [23], differential quadrature hierarchical finite element method [24], asymptotic integration method [25] and Galerkin method [26,27]. Each of these methods has its own advantages and shortcomings. Here the generalised differential quadrature method is used to discrete the motion and energy equations through the radius of the hollow sphere. Applying the generalised differential quadrature method to Eq. (17) results in the following non-linear time-dependent equations.

The descretized form the of the equation of motion is:

$$\begin{aligned} &\sum_{j=1}^{N} \left(C_{ij}^{(2)} + \left(\frac{2}{\hat r_i} + \frac{\lambda_E}{\hat c} \right) C_{ij}^{(1)} + 2\left(-\frac{1}{\hat r_i^2} + \frac{\lambda_E \nu}{\hat r_i \hat c (1-\nu)} \right) C_{ij}^{(0)} \right) u_j - \\ &\sum_{j=1}^{N} e^{\lambda_\alpha \frac{\hat r_i - \hat a}{\hat c}} \left(C_{ij}^{(1)} + \left(\frac{\lambda_E + \lambda_\alpha}{\hat c} \right) C_{ij}^{(0)} \right) \theta_j - \sum_{j=1}^{N} \left(e^{(\lambda_\rho - \lambda_E)\frac{\hat r_i - \hat a}{\hat c}} C_{ij}^{(0)} \right) \ddot u_j = 0 \end{aligned} \tag{20}$$

and the descretized form of the energy equation is expressed as:

$$\sum_{j=1}^{N}\left(C_{ij}^{(2)}+\left(\frac{2}{\hat{r}_i}+\frac{\lambda_K}{\hat{c}}\right)C_{ij}^{(1)}\right)\theta_j-\sum_{j=1}^{N}\left(e^{\left(\lambda_{C_e}+\lambda_\rho-\lambda_K\right)\frac{\hat{r}_i-\hat{a}}{\hat{c}}}C_{ij}^{(0)}\right)\dot{\theta}_j-$$
$$\hat{t}_0\sum_{j=1}^{N}\left(e^{\left(\lambda_{C_e}+\lambda_\rho-\lambda_K\right)\frac{\hat{r}_i-\hat{a}}{\hat{c}}}C_{ij}^{(0)}\right)\ddot{\theta}_j-A\hat{t}_0\sum_{j=1}^{N}\left(e^{\left(\lambda_E+\lambda_\alpha-\lambda_K\right)\frac{\hat{r}_i-\hat{a}}{\hat{c}}}C_{ij}^{(0)}\right)\dot{\theta}_j\sum_{j=1}^{N}\left(C_{ij}^{(1)}+\frac{2}{\hat{r}_i}C_{ij}^{(0)}\right)\dot{u}_j-$$
$$A\left(1+\sum_{j=1}^{N}C_{ij}^{(0)}\theta_j\right)\times$$
$$\left[\sum_{i=1}^{N}e^{\left(\lambda_E+\lambda_\alpha-\lambda_K\right)\frac{\hat{r}_i-\hat{a}}{\hat{c}}}\left(C_{ij}^{(1)}+\frac{2}{\hat{r}_i}C_{ij}^{(0)}\right)\dot{u}_j+\hat{t}_0\sum_{j=1}^{N}e^{\left(\lambda_E+\lambda_\alpha-\lambda_K\right)\frac{\hat{r}_i-\hat{a}}{\hat{c}}}\left(C_{ij}^{(1)}+\frac{2}{\hat{r}_i}C_{ij}^{(0)}\right)\ddot{u}_j\right]=0 \tag{21}$$

where in the above equations, $C_{ij}^{(r)}$'s are the weighting coefficients associated with the $r-$ th derivative and N is the number of grid points. Furthermore, r_i is the position of $i-$ th node in the GDQ method. Distribution of the points is based on the well-known Chebyshev-Gauss-Lobatto method. For the case when the inner and outer radii of the sphere in non-dimensional form are denoted, respectively, by $\hat{a}$ and $\hat{b}$, distribution of the points is obtained as

$$\hat{r}_i=\frac{\hat{a}+\hat{b}}{2}+\frac{\hat{a}-\hat{b}}{2}\cos\left(\frac{i-1}{N-1}\pi\right), i=1,2,\ldots,N \tag{22}$$

The system of equations (20) and (21) in a matrix form may be represented as

$$\begin{bmatrix} M^{uu} & M^{u\theta} \\ M^{\theta u} & M^{\theta\theta}\end{bmatrix}\begin{Bmatrix}\ddot{u}\\ \ddot{\theta}\end{Bmatrix}+\begin{bmatrix} M^{uu} & M^{u\theta} \\ M^{\theta u} & M^{\theta\theta}\end{bmatrix}\begin{Bmatrix}\dot{u}\\ \dot{\theta}\end{Bmatrix}+\begin{bmatrix} K^{uu} & K^{u\theta} \\ K^{\theta u} & K^{\theta\theta}\end{bmatrix}\begin{Bmatrix}u\\ \theta\end{Bmatrix}=\begin{Bmatrix}F^{u}\\ F^{\theta}\end{Bmatrix} \tag{23}$$

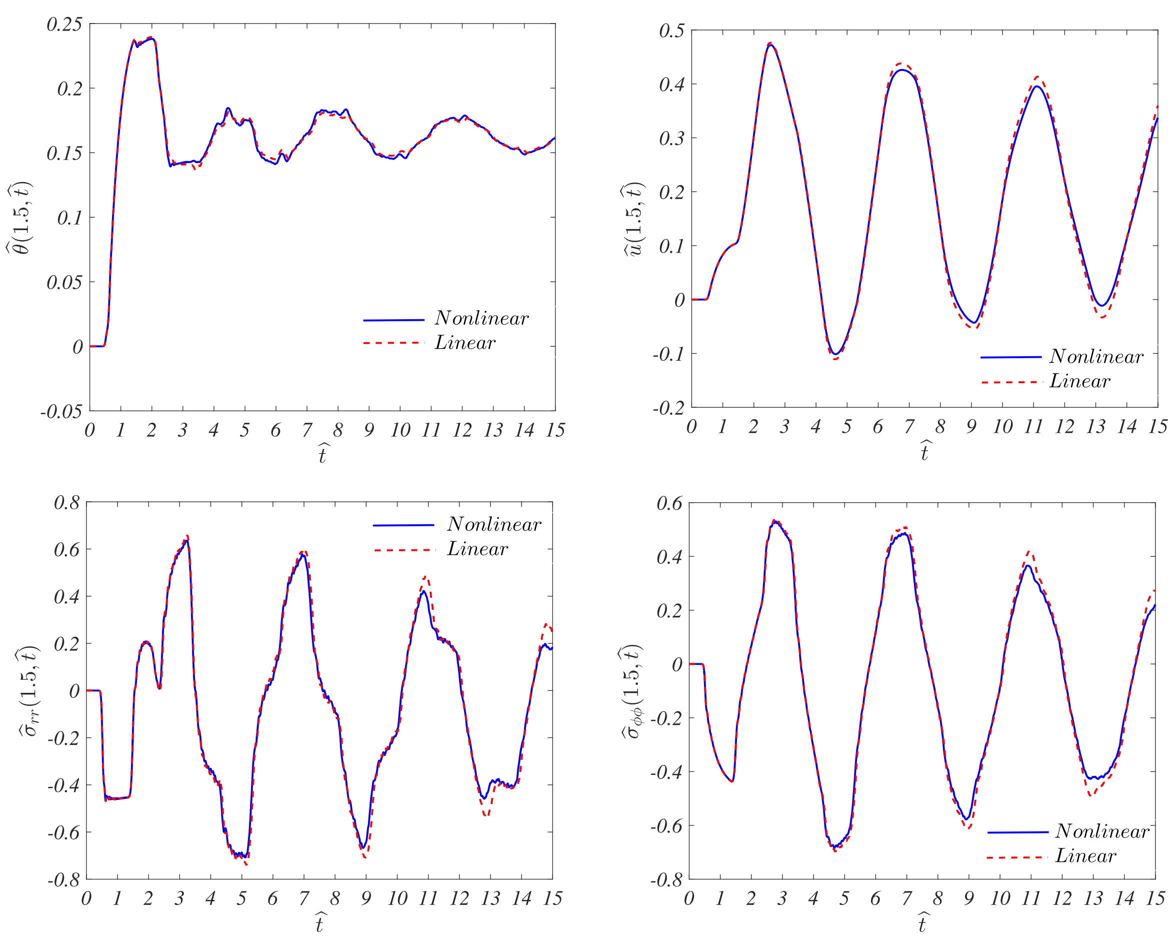

Fig. 5. Linear and nonlinear temporal evolution of dimensionless radial displacement, temperature, radial and hoop stresses at $\hat{r}=1.5$ of an FGM hollow sphere with $\hat{t}_0=1$, $\lambda=1$, $A=0.02111$ and $\hat{q}_{in}=2$.

where the elements of mass matrix, damping matrix, stiffness matrix and force vector are as

$$
\begin{aligned}
&M_{ij}^{uu}=-\left(e^{(\lambda_\rho-\lambda_E)\frac{\hat r_i-\hat a}{\hat c}}\right)C_{ij}^{(0)}\\
&M_{ij}^{u\theta}=0\\
&C_{ij}^{uu}=0\\
&C_{ij}^{u\theta}=0\\
&K_{ij}^{uu}=C_{ij}^{(2)}+\left(\frac{2}{\hat r_i}+\frac{\lambda_E}{\hat c}\right)C_{ij}^{(1)}+2\left(-\frac{1}{\hat r_i^2}+\frac{\nu\lambda_E}{\hat r_i\hat c(1-\nu)}\right)C_{ij}^{(0)}\\
&K_{ij}^{u\theta}=-e^{\lambda_\alpha\frac{\hat r_i-\hat a}{\hat c}}\left(C_{ij}^{(1)}+\left(\frac{\lambda_E+\lambda_\alpha}{\hat c}\right)C_{ij}^{(0)}\right)\\
&M_{ij}^{\theta u}=-A\hat t_0(1+\theta_j)e^{(\lambda_E+\lambda_\alpha-\lambda_K)\frac{\hat r_i-\hat a}{\hat c}}\left(C_{ij}^{(1)}+\frac{2}{\hat r_i}C_{ij}^{(0)}\right)\\
&M_{ij}^{\theta\theta}=-\hat t_0e^{\left(\lambda_{C_\epsilon}+\lambda_\rho-\lambda_K\right)\frac{\hat r_i-\hat a}{\hat c}}C_{ij}^{(0)}\\
&C_{ij}^{\theta u}=-A\left(1+\theta_j+\hat t_0\dot\theta_j\right)e^{(\lambda_E+\lambda_\alpha-\lambda_K)\frac{\hat r_i-\hat a}{\hat c}}\left(C_{ij}^{(1)}+\frac{2}{\hat r_i}C_{ij}^{(0)}\right)\\
&C_{ij}^{\theta\theta}=-e^{\left(\lambda_{C_\epsilon}+\lambda_\rho-\lambda_K\right)\frac{\hat r_i-\hat a}{\hat c}}C_{ij}^{(0)}\\
&K_{ij}^{\theta u}=0\\
&K_{ij}^{\theta\theta}=C_{ij}^{(2)}+\left(\frac{2}{\hat r_i}+\frac{\lambda_K}{\hat c}\right)C_{ij}^{(1)}\\
&F_i^u=0\\
&F_i^\theta=0
\end{aligned}
\tag{24}
$$

Similar to the governing equations, the GDQ method should be applied to the boundary conditions. As mentioned earlier, it is assumed that the non-dimensional inner and outer radii of the sphere are, respectively, $\hat a$ and $\hat b$. The following boundary conditions are used for inner and outer radii of the sphere as

$$
\begin{aligned}
&\hat r=\hat a:\hat u=0\,,\ -\frac{\partial\hat\theta}{\partial\hat r}=\hat q_{in}\\
&r=\hat b:\hat\sigma_{rr}=0,\ \hat\theta=0
\end{aligned}
\tag{25}
$$

The above boundary conditions express a hollow sphere which is subjected to thermal shock at inner surface, while outer surface is kept at reference temperature. Furthermore, the outer surface is free of radial stress and the inner surface is free of radial deformation. Upon application of the GDQ method, Eq. (25) takes the form

$$
\begin{aligned}
&\hat r=\hat r_1:\sum_{j=1}^{N}C_{1j}^{(0)}u_j=0,\sum_{j=1}^{N}C_{1j}^{(1)}\theta_j=-\hat q_{in}\\
&\hat r=\hat r_N:\sum_{j=1}^{N}e^{\lambda_E}\left(C_{Nj}^{(1)}+\frac{2\nu}{\hat b(1-\nu)}C_{Nj}^{(0)}\right)u_j-\sum_{j=1}^{N}e^{\lambda_E+\lambda_\alpha}C_{Nj}^{(0)}\theta_j=0,\sum_{j=1}^{N}C_{Nj}^{(0)}\theta_j=0
\end{aligned}
\tag{26}
$$

Various methods are available to apply the boundary conditions to the discreted motion and energy equations. In this study, boundary conditions (26) are applied directly to Eq. (23). After that, the motion and energy equations may be written as

$$\mathbf{M}(\mathbf{X})\ddot{\mathbf{X}}+\mathbf{C}(\mathbf{X},\dot{\mathbf{X}})\dot{\mathbf{X}}+\mathbf{K}\mathbf{X}=\mathbf{F} \tag{27}$$

To complete the approximation, one should approximate the time derivatives in Eq. (27). Here, the Newmark direct integration scheme based on the constant average acceleration method ($\alpha_N=0.5,\beta_N=0.25$) is applied [28,29]. Implementation of the Newmark method to Eq. (27) yields

$$\widehat{\mathbf{K}}(\mathbf{X})\mathbf{X}_{j+1}=\widehat{\mathbf{F}}_{j,j+1} \tag{28}$$

where

$$
\begin{aligned}
&\widehat{\mathbf{K}}_{j+1}=\mathbf{K}_{j+1}+a_3\mathbf{M}_{j+1}+a_6\mathbf{C}_{j+1}\\
&\widehat{\mathbf{F}}_{j,j+1}=\mathbf{F}_{j+1}+\mathbf{M}_{j+1}\left(a_3\mathbf{X}_j+a_4\dot{\mathbf{X}}_j+a_5\ddot{\mathbf{X}}_j\right)+\mathbf{C}_{j+1}\left(a_6\mathbf{X}_j+a_7\dot{\mathbf{X}}_j+a_8\ddot{\mathbf{X}}_j\right)
\end{aligned}
\tag{29}
$$

with

$$
\begin{aligned}
&a_1=\alpha_N\Delta t,\ a_2=(1-\alpha_N)\Delta t\\
&a_3=\frac{1}{\beta_N\Delta t^2},\ a_4=\frac{1}{\beta_N\Delta t},\ a_5=\frac{1-2\beta_N}{2\beta_N}\\
&a_6=\frac{\alpha_N}{\beta_N\Delta t},\ a_7=\frac{\alpha_N-\beta_N}{\beta_N},\ a_8=\frac{\alpha_N-2\beta_N}{2\beta_N}\Delta t
\end{aligned}
\tag{30}
$$

Once the solution $\mathbf{X}$ is known at $t_{j+1}=(j+1)\Delta t$, the first and second derivatives of $\mathbf{X}$ at t_{j+1} can be computed from

$$
\begin{aligned}
&\ddot{\mathbf{X}}_{j+1}=a_3\left(\mathbf{X}_{j+1}-\mathbf{X}_j\right)-a_4\dot{\mathbf{X}}_j-a_5\ddot{\mathbf{X}}_j\\
&\dot{\mathbf{X}}_{j+1}=\dot{\mathbf{X}}_j+a_2\ddot{\mathbf{X}}_j+a_1\ddot{\mathbf{X}}_{j+1}
\end{aligned}
\tag{31}
$$

The resulting equation (28) are solved at each time step using the information known from the preceding time step solution. At time $t=0$, the initial values of $\mathbf{X}$, $\dot{\mathbf{X}}$, and $\ddot{\mathbf{X}}$ are known or obtained by solving Eq. (27) at time $t=0$ and are used to initiate the time marching procedure. Since the hollow sphere is initially at rest, the initial values of $\mathbf{X}$ and $\dot{\mathbf{X}}$ are assumed to be zero. In other words, the initial conditions to begin the time marching are

$$\hat u(r,0)=\dot{\hat u}(r,0)=\hat\theta(r,0)=\dot{\hat\theta}(r,0)=0 \tag{32}$$

An iterative scheme should be applied to Eq. (28) to solve the resulting nonlinear algebraic equations. In this study, the well-known Picard iterative scheme is used. Details of the Picard scheme are not presented herein for the sake of brevity, meanwhile one may refer to Ref. [28].

7. Results and discussion

A hollow sphere made of an exponentially graded material is assumed in the present research. The inner side of the sphere is made from Aluminum with properties $E_0=70$GPa, $\nu=0.3$, $\alpha_0=23\times10^{-6}$1/K, $\rho_0=2707$kg/m^3, $K_0=204$W/m and $C_{\epsilon0}=903$ J/kg.K. The dimensionless inside and outside radii of the hollow sphere, are, respectively $\hat a=1$ and $\hat b=2$. Unless otherwise mentioned, the boundary conditions are similar with those provided in Eq. (25). In the next, at first a comparison study is given between the results of this study and those given by other researchers. After that novel numerical results from the present research are given. In the results of this section, it is assumed that all of the FG indices are the same, i.e., $\lambda=\lambda_E=\lambda_\rho=\lambda_{C_\epsilon}=\lambda_K=\lambda_\alpha$. The reference temperature is set equal to $T_0=300$K for all of this section. The number of grid points in the GDQ method is set equal to $N=201$. Also the time step of the Newmark method is set equal to $\Delta t=0.001$.

7.1. Comparison study

A comparison study is performed in this section for the case of a hollow sphere made from an isotropic homogeneous material. This can be done easily when all of the indices of the FGM sphere are set equal to zero, i.e. $\lambda=0$. For the sake of the comparison, the following quantities are used. Relaxation time in dimensionless presentation is set equal to one, $\hat t_0=1$. The coupling parameter is set equal to $A=0.02111$. This is the real value of coupling parameter which is evaluated at reference

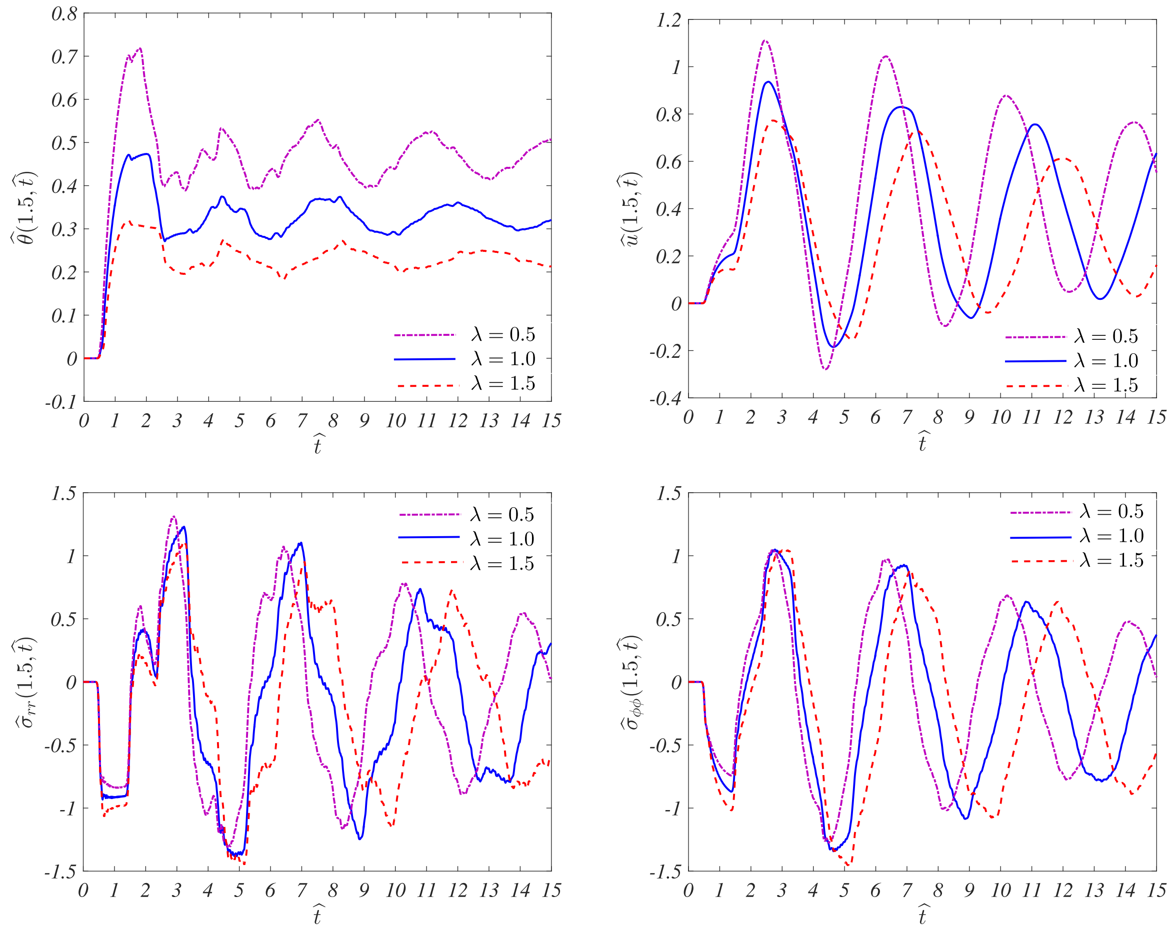

Fig. 6. Nonlinear temporal evolution of dimensionless radial displacement, temperature, radial and hoop stresses at $\hat{r} = 1.5$ of an FGM hollow sphere with $\hat{t}_0 = 1$, $A = 0.02111$, $\hat{q}_{in} = 4$ and various λ indices.

temperature $T = 300$K. The inside surface of the sphere is subjected to a shock of magnitude $\hat{q}_{in} = 4$. For the sake of comparison, thermally non-linear based temporal evolution of displacement, temperature and stresses are obtained at $\hat{r} = 1.5$. Results are depicted in Fig. (1) and compared with those of Kiani and Eslqmi [30]. It is seen that, excellent agreement is achieved between the results of this study and those of Kiani and Eslami [30] which accepts the correctness and efficiency of the developed formulation and solution method.

7.2. Parametric studies

After validating the present formulation and solution method with the available data in the open literature, novel numerical results are given in this section.

7.2.1. Importance of non-linearity

For the fist study, the importance of non-linear analysis is depicted. Results of this study are provided in Fig. (2). For generating the numerical results of this figure, a spherical vessel with $\hat{t}_0 = 1$, $A = 0.02111$, $\lambda = 1$ and $\hat{q}_{in} = 4$ is assumed. Temporal evolution of dimensionless radial displacement, temperature, radial and azimuthal stresses are depicted in Fig. (2) based on both linear and non-linear analysis. It is seen that, under the thermally non-linear analysis, the magnitudes of both stresses and displacement alleviate. The differences of temperature profiles obtained by thermally linear and non-linear analysis are hardly distinguishable. It is also seen that the magnitudes of stresses, displacement and temperature at $\hat{r} = 1.5$ are equal to zero up to a certain time. This feature accepts the fact that all of these waves propagate with finite speed.

7.2.2. Importance of coupling parameter

To discuss the importance of coupling parameter, a study is performed in this section and its results are provided in Fig. (3). For this aim, all of the parameters are the same with those used in Fig. (2) except for the coupling parameter which is set equal to $A = 0.05$. Consequently, one may obtain the influence of this parameter on the propagation of waves via the comparison of results in Fig. (2) and Fig. (3). Comparison of these two figures accept the fact that, as the coupling parameter increases, the divergence of the results between the thermally linear and non-linear theories enhances. Therefore for higher magnitudes of coupling parameter the adoption of thermally nonlinear analysis is inevitable.

7.2.3. Importance of thermal relaxation time

Results of Fig. (4) aim to analyse the effects of thermal relaxation time on the temporal evolution of displacement, temperature and stresses within a hollow sphere. To this aim, a spherical vessel with properties similar to those used in Fig. (2) are considered except for the thermal relaxation time which is set equal to $\hat{t}_0 = 0.36$. Therefore a smaller value of thermal relaxation time is used in comparison to the one used in Fig. (2). It is seen that divergence of the results obtained by the linear and nonlinear analysis enhances with an increase in the thermal relaxation time. Therefore for high values of thermal relaxation time the use of thermally nonlinear analysis is unavoidable.

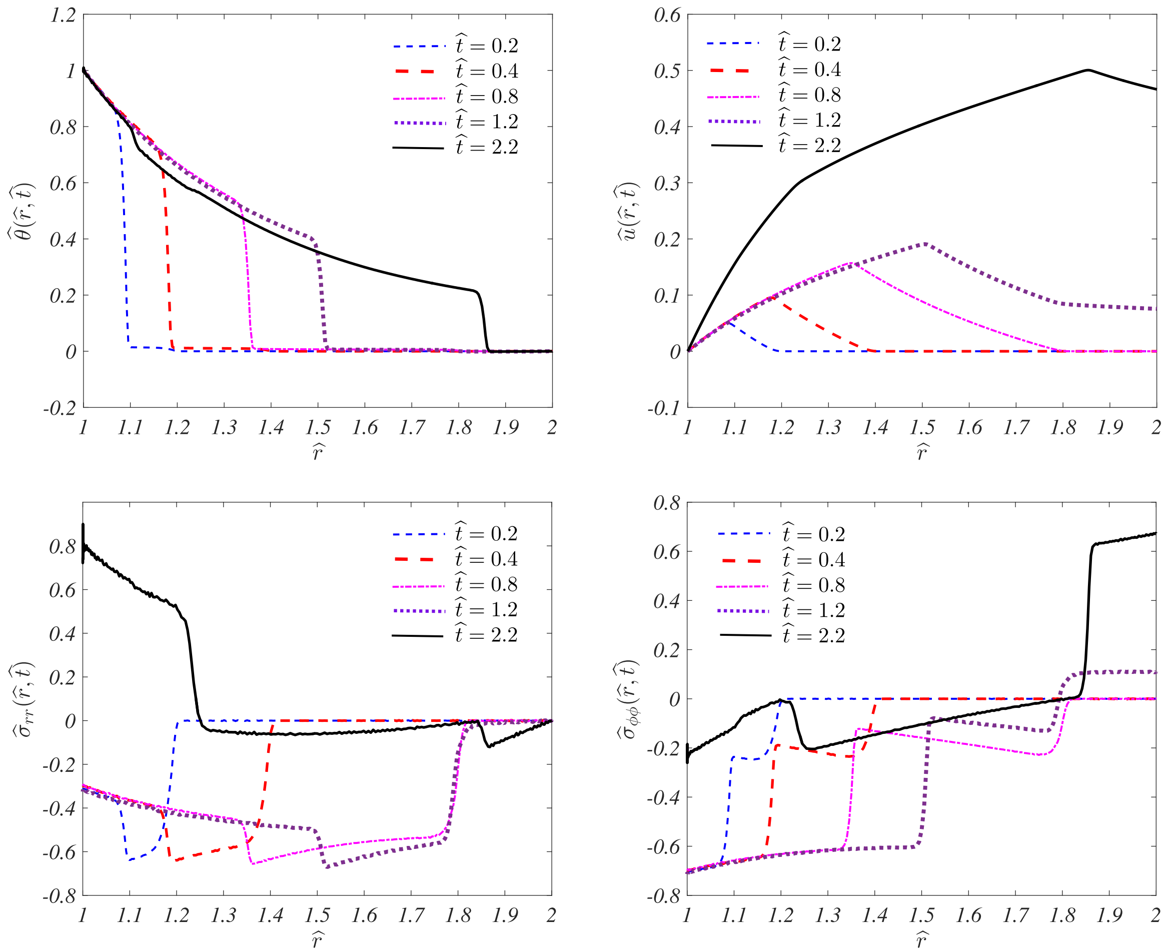

Fig. 7. Propagation of radial displacement, temperature, radial and hoop stress waves at different times for an FGM hollow sphere with $\hat{t}_0 = 4, \lambda = 1, A = 0.02111$ and $\hat{\theta}_{in} = 4$.

7.2.4. Importance of thermal shock

Results of Fig. (5) aim to discuss the effects of magnitude of thermal shock on the thermally nonlinear temporal evolution of displacement, temperature and stresses. In generating the results of this figure, all of the parameters are the same with those used in Fig. (2) except for the thermal shock magnitude which is set equal to $\hat{q}_{in} = 2$. As seen from the comparison of results of Fig. (2) and Fig. (5), higher magnitudes of shock results in higher divergence between the thermally nonlinear- and thermally linear-based results. This is expected since as the magnitude of shock enhances, temperature within the body increases. Under such condition, the assumption of small temperature change in comparison to reference temperature becomes poor and therefore non-linear analysis should be performed.

7.2.5. Importance of exponential index

Figure (6) depicts the effect of exponential index of the functionally graded media. To this aim spherical vessels with material properties $\hat{t}_0 = 1, A = 0.02111, \hat{q}_{in} = 4$ are considered. Three different values are considered for FGM index which are $\lambda = 0.5, 1$ and 1.5. Temporal evolution of temperature, displacement and stresses are obtained and depicted in Figure (6). It is seen that as the exponential index of the FGM vessel increases, the radial displacement in the vessel decreases. This is due to the fact that increasing the exponential index of the FGM vessel enhances the stiffness of the vessel which leads to the lower displacement. Also temperature within the body decreases as the exponential index enhances. The effect of graded pattern of the FG vessel on the stresses is not comparable with respect to its effect on temperature and displacement.

7.2.6. Propagation of waves

An example on the type of thermal shock is depicted in Fig. 7. All of the boundary conditions are the same with those defined in (25) except for the type of thermal shock. Instead of heat flux in this example the sudden temperature elevation is exposed to the inner edge of the hollow sphere. The applied thermal shock is considered in the form

$$\hat{\theta} = \hat{\theta}_{in}\left(1 - (1 + 100\hat{t})e^{-100\hat{t}}\right) \tag{33}$$

Figure (7) demonstrates the propagation of thermal and mechanical waves at different times in the sphere. A hollow sphere with material properties $\hat{t}_0 = 4, \lambda = 1, A = 0.02111$ which is subjected to the shock of magnitude $\hat{\theta}_{in} = 4$ is assumed. Based on the thermally non-linear analysis, propagation of waves at $\hat{t} = 0.2$, 0.4, 0.8, 1.2 and 2.2 is provided. As seen from the results, temperature propagates with finite speed which is the main conclusion from the Lord-Shulman theory assumption. It is also seen that this theory admits the energy dissipation. The speed of temperature wave in the body is not constant since the properties are position dependent. This is also compatible with the observation of Figure (7) since the temperature wave front is located at $\hat{r} = 1.1$ and 1.5 for $\hat{t} = 0.2$ and 1.2. The induced stresses in the vessel are both compressive at the initial steps of heating since one surface of the vessel is restrained against expansion. In the portraits of stresses, two

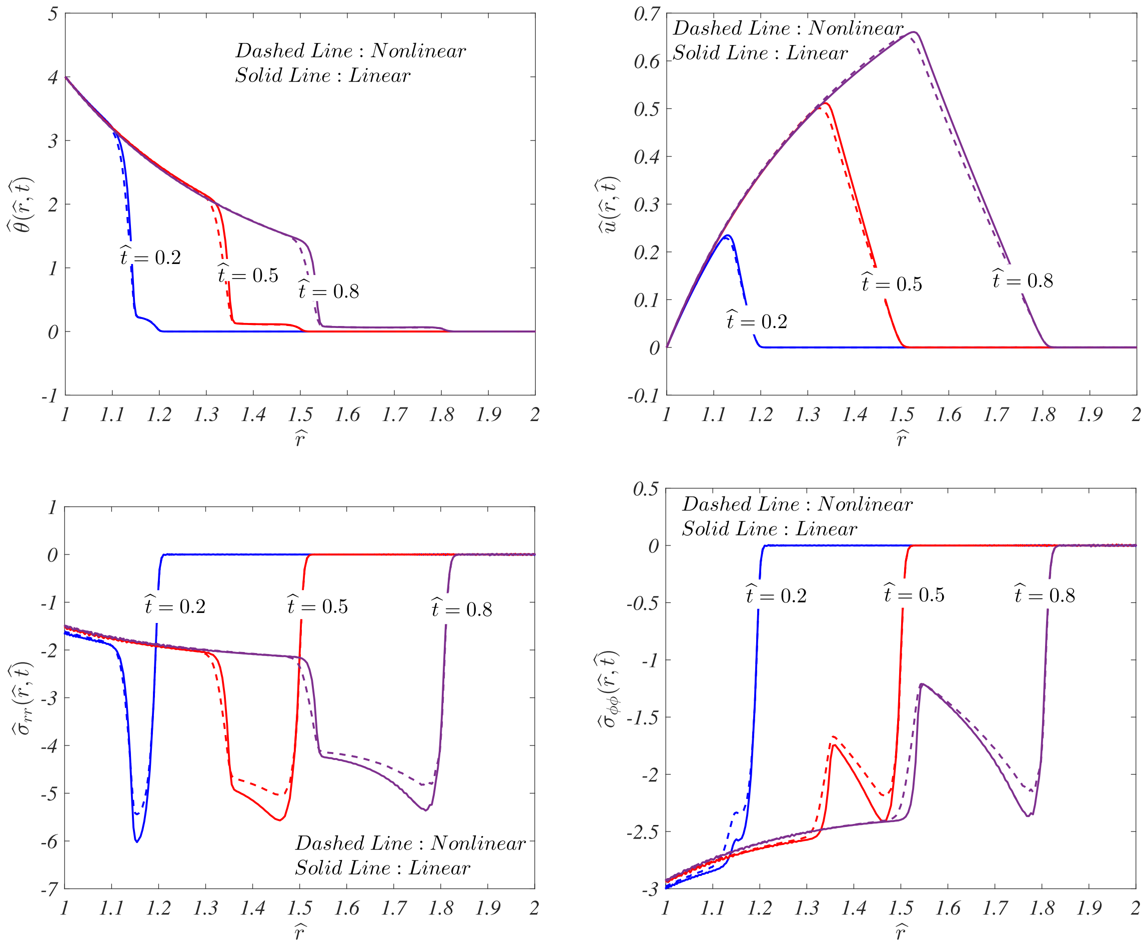

Fig. 8. Propagation of radial displacement, temperature, radial and hoop stress waves at different times for an FGM sphere with $\hat{t}_0 = 1.5625$, $\lambda = 1$, $A = 0.02111$ and $\hat{\theta}_{in} = 4$.

discontinuities are observed. The first one is attributed to temperature wave front and the second one is attributed to displacement wave front. For $\hat{t} = 2.2$, the radial displacement wave is reached to the other side of the vessel, reflected back and again reached to the inner side of the vessel and reflected back.

Finally an attempt is made to show the importance of thermally nonlinear analysis on the propagation of waves. For three different times, the portraits of waves is provided. Properties of the vessel are $\hat{t}_0 = 1.5625$, $\lambda = 1$, $A = 0.02111$ and $\hat{\theta}_{in} = 4$. Results are depicted in Fig. (8). It is seen that, under thermally nonlinear analysis, the magnitudes of stresses and displacement are underestimated.

8. Conclusion

Generalised thermo-elasticity response of a hollow sphere made from an exponentially graded material is considered in this research. The Lord and Shulman theory of thermo-elasticity is used to consider the finite speed and temperature wave propagation. Two coupled equations, namely the equation of motion and energy equation are established. The energy equation, unlike many of the other available works is kept in its nonlinear form and the linearization of the previous works is not performed in this research. The obtained coupled and nonlinear equations are provided in a dimensionless presentation. After that, with the aid of the GDQ method and Newmark time marching scheme, a system of nonlinear algebraic equations is achieved. Picard algorithm is used to obtain the magnitudes of displacement, stresses and temperature at each time. It is concluded that, under thermally nonlinear analysis, stresses and displacement are underestimated. Also as the coupling parameter, thermal relaxation time or magnitude of shock increases, the use of thermally nonlinear analysis becomes more important.

Author statement

Peyman Karimi Zeverdejani: Investigation; Methodology; Validation; Writing - original draft; Writing - review & editing. Yaser Kiani: Investigation; Methodology; Validation; Writing - original draft; Writing - review & editing.

Declaration of competing interest

The author of this study declare that they have no conflict of interest.

Acknowledgement

This work has been financially supported by the research deputy of Shahrekord University. The Grant Number was 97GRN1M40504.

References

[1] J. Zhang, A. Oueslati, W.Q. Shen, G. de Saxcé, Exact elastic solution of the axisymmetric and deviatoric loaded hollow sphere, Int. J. Pres. Ves. Pip. 162 (No. 1) (2018) 40–45.
[2] M.R. Eslami, M.H. Babaei, R. Poultangari, Thermal and mechanical stresses in a functionally graded thick sphere, Int. J. Pres. Ves. Pip. 82 (No. 7) (2005) 522–527.
[3] R. Poultangari, M. Jabbari, M.R. Eslami, Functionally graded hollow spheres under non-axisymmetric thermo-mechanical loads, Int. J. Pres. Ves. Pip. 85 (No. 5) (2008) 295–305.
[4] A. Kar, M. Kanoria, Generalized thermoelastic functionally graded orthotropic hollow sphere under thermal shock with three-phase-lag effect, Eur. J. Mech. Solid. 28 (No. 4) (2009) 757–767.
[5] M. Shariyat, S. Jahanshahi, H. Rahimi, Nonlinear Hermitian generalized hygrothermoelastic stress and wave propagation analyses of thick FGM spheres exhibiting temperature, moisture, and strain-rate material dependencies, Compos. Struct. 229 (2019). Article Number 111364.
[6] Y. Heydarpour, P. Malekzadeh, F. Gholipour, Thermoelastic analysis of FG-GPLRC spherical shells under thermo-mechanical loadings based on Lord-Shulman theory, Compos. B Eng. 164 (2019) 400–424.
[7] S. Banik, M. Kanoria, Effects of three-phase-lag on two-temperature generalized thermoelasticity for infinite medium with spherical cavity, Appl. Math. Mech. 33 (No. 4) (2012) 483–498.
[8] A. Bagri, M.R. Eslami, A unified generalized thermoelasticity; solution for cylinders and spheres, Int. J. Mech. Sci. 49 (No. 12) (2007) 1325–1335.
[9] A. R Shahani, S. Momeni Bashusqeh, Analytical solution of the thermoelasticity problem in a pressurized thick-walled sphere subjected to transient thermal loading, Math. Mech. Solid 19 (No. 2) (2014) 135–151.
[10] A. R Shahani, S. Momeni Bashusqeh, Analytical solution of the coupled thermo-elasticity problem in a pressurized sphere, J. Therm. Stresses 36 (No. 12) (2013) 1283–1307.
[11] Y. Povstenko, Dirichlet problem for time-fractional radial heat conduction in a sphere and associated thermal stresses, J. Therm. Stresses 34 (1) (2011) 51–67.
[12] Y. Povstenko, Time-fractional thermoelasticity problem for a sphere subjected to the heat flux, Appl. Math. Comput. 257 (2015) 327–334.
[13] A. Sur, M. Kanoria, Fractional heat conduction with finite wave speed in a thermo-visco-elastic spherical shell, Lat. Am. J. Solid. Struct. 11 (No. 7) (2014) 1132–1162.
[14] R.B. Hetnarski, M.R. Eslami, Thermal Stresses, Advanced Theory and Applications, Springer, Amsterdam, 2009.
[15] N. Noda, R.B. Hetnarski, Y. Tanigawa, Thermal Stresses, CRC Press, New York, 2003.
[16] T.C.K. Molyneaux, L.Y. Li, Instability of cylindrical panels under combined static and dynamic loads, Int. J. Pres. Ves. Pip. 65 (No. 2) (1996) 163–169.
[17] M. Shariyat, D. Asgari, Nonlinear thermal buckling and postbuckling analyses of imperfect variable thickness temperature-dependent bidirectional functionally graded cylindrical shells, Int. J. Pres. Ves. Pip. 111–112 (2013) 310–320.
[18] O. Civalek, Linear vibration analysis of isotropic conical shells by discrete singular convolution (DSC), Struct. Eng. Mech. 25 (No. 1) (2007) 127–130.
[19] O. Civalek, Vibration analysis of conical panels using the method of discrete singular convolution, Commun. Numer. Methods Eng. 24 (No. 3) (2008) 169–181.
[20] O. Civalek, M.H. Acar, Discrete singular convolution method for the analysis of Mindlin plates on elastic foundations, Int. J. Pres. Ves. Pip. 84 (No. 9) (2007) 527–535.
[21] B. Akgoz B, O. Civalek, Nonlinear vibration analysis of laminated plates resting on nonlinear two-parameters elastic foundations, Steel Compos. Struct. 11 (No. 5) (2011) 403–421.
[22] G.H. Nie, Analysis of non-linear behaviour of imperfect shallow spherical shells on pasternak foundation by the asymptotic iteration method, Int. J. Pres. Ves. Pip. 80 (No. 4) (2003) 229–235.
[23] O. Civalek, Geometrically nonlinear dynamic analysis of doubly curved isotropic shells resting on elastic foundation by a combination of harmonic differential quadrature-finite difference methods, Int. J. Pres. Ves. Pip. 82 (No 6) (2005) 470–479.
[24] Y. Wu, Y. Xing, B. Liu, Analysis of isotropic and composite laminated plates and shells using a differential quadrature hierarchical finite element method, Compos. Struct. 205 (2018) 11–25.
[25] N.K. Akhmedovam, A.H. Sofiyev, Asymptotic analysis of three-dimensional problem of elasticity theory for radially inhomogeneous transversally-isotropic thin hollow spheres, Thin-Walled Struct. 139 (2019) 232–241.
[26] A.H. Sofiyev, P. Ozyigit, Thermal buckling analysis of non-homogenous shallow spherical shells, Journal of the Faculty of Engineering and Architecture of Gazi University 27 (2012) 397–405.
[27] A.H. Sofiyev, N. Kuruoglu, Non-linear buckling of an FGM truncated conical shell surrounded by an elastic medium, Int. J. Pres. Ves. Pip. 107 (2013) 38–49.
[28] D.W. Pepper, The Intermediate Finite Element Method, CRC Press, New York, 1999.
[29] M.R. Eslami, Finite Elements Methods in Mechanics, Springer, 2014.
[30] Y. Kiani, M.R. Eslami, The GDQ approach to thermally nonlinear generalized thermoelasticity of a hollow sphere, Int. J. Mech. Sci. 118 (No. 1) (2016) 195–204.